

**Geometric optimal control and two-level dissipative quantum systems\***

by

**Bernard Bonnard<sup>1</sup> and Dominique Sugny<sup>2</sup>**

<sup>1</sup> Institut de Mathématiques de Bourgogne, UMR CNRS 5584  
9 Avenue Alain Savary, BP 47 870, F-21078 Dijon Cedex, France

<sup>2</sup> Institut Carnot de Bourgogne, UMR 5209 CNRS-Université de Bourgogne  
9 Avenue Alain Savary, BP 47 870, F-21078 Dijon Cedex, France

**Abstract:** The objective of this article is to present techniques of geometric time-optimal control developed to analyze the control of two-level dissipative quantum systems. Combined with numerical simulations they allow to compute the time-minimal control using a shooting method. The robustness with respect to initial conditions and dissipative parameters is also analyzed using a continuation method.

**Keywords:** optimal control theory, conjugate and cut loci, quantum mechanics.

## 1. Introduction

The use of recent geometric control techniques to analyze quantum control systems is a new challenge in optimal control theory. In this context, many articles are devoted to the conservative case, see, e.g., Boscain et al. (2002), Khaneja, Brockett and Glaser (2001, 2002). In this study, we extend these works to the *dissipative* case and we concentrate on two-level systems. We present a complete analysis of this case based on our recent works Sugny, Kontz and Jauslin (2007), Bonnard and Sugny (2009a) and Bonnard, Chyba and Sugny (2009), which are illustrated by numerical simulations. This study is also motivated by the ANR research experimental project CoMoc, where the goal is to control the rotation of molecules in a gas phase by laser fields. Additional dissipation terms due to molecular collisions can also be introduced in the model (see Vieillard et al., 2008). Although our analysis is restricted to the two-level case, the techniques can be used combined with numerical simulations, to analyze more realistic systems, where about twenty or more levels have to be taken into account. Also it is a good opportunity to present methods of geometric control in an article

---

\*Submitted: October 2008; Accepted March 2009.

written for the 50 years of optimal control in order to analyze complex systems originating from control engineering.

From the description given in Bonnard and Sugny (2009b), we assume that the dynamics of the system is governed by the Kossakowski-Lindblad equation and that the control is given by the complex Rabi frequency of the laser field. Using the rotating wave approximation, the equations can be written in suitable coordinates as follows

$$\begin{cases} \dot{x} = -\Gamma x + u_2 z \\ \dot{y} = -\Gamma y - u_1 z \\ \dot{z} = \gamma_- - \gamma_+ z + u_1 y - u_2 x \end{cases} \quad (1)$$

where the state space  $q = {}^t(x, y, z)$  belongs to the Bloch ball  $|q| \leq 1$ , which is invariant for the dynamics considered;  $\Lambda = (\Gamma, \gamma_+, \gamma_-)$  is the set of parameters satisfying the constraints  $2\Gamma \geq \gamma_+ \geq |\gamma_-|$  and the control is  $u = |u|e^{i\alpha} = u_1 + iu_2$  with bounded amplitude which can be normalized to 1.

We consider the time-minimal transfer from a state  $q_0$  to a state  $q_1$ . Hence we have to analyze a time-minimal problem for a control system of the form

$$\frac{dq}{dt} = F_0(q) + \sum_{i=1}^2 u_i F_i(q), |u| \leq 1,$$

where the drift term  $F_0$  depends upon three parameters and the vector fields  $F_i$  are affine. This control problem is a very difficult problem, whose analysis requires developments of geometric optimal control theory and numerical simulations.

The organization of this article is the following. In Section 2, we present properties of time-minimal control for systems of the form

$$\frac{dq}{dt} = F_0(q) + \sum_{i=1}^m u_i F_i(q), q \in \mathbb{R}^n, u = (u_1, \dots, u_m), |u| \leq 1. \quad (2)$$

This problem is a generalization of a *Zermelo navigation problem* (see Bao, Robles and Shen, 2004, and Carathéodory, 1982) which corresponds to a situation where the number of inputs is equal to the dimension of the state and where the vector fields  $F_i, i = 1, \dots, m$  are linearly independent. The Pontryagin maximum principle (Pontryagin et al., 1961) applied to this generalized Zermelo navigation problem is used to split the analysis into two distinct parts. First of all, we consider generic extremal trajectories, where the control is given by  $u_i = H_i / \sqrt{\sum_{i=1, m} H_i^2}$  and  $H_i$  is the Hamiltonian  $\langle p, F_i \rangle$ ; such trajectories are smooth curves, solutions of the Hamiltonian vector field  $\vec{H}_r$  where  $H_r = H_0 + (\sum_{i=1, m} H_i^2)^{1/2}$ . Secondly, we must analyze the singularities due to the existence of a switching surface  $\Sigma : H_i = 0, i = 1, \dots, m$ , where we can connect solutions of the Hamiltonian vector field  $\vec{H}_r$ . The connection rules are given by the maximum principle which generalizes the Erdman-Weierstrass

condition from the standard calculus of variations. From this point of view, the switchings are related to a singularity analysis associated to the Hamiltonian vector field  $\vec{H}_r$  (see Ekeland, 1978). An important remark is then to observe that the solutions associated to  $\vec{H}_r$  correspond to extremal solutions if we restrict the control domain to the sphere  $S^{m-1} : |u| = 1$ . An instant of reflexion shows that complicated singularities can occur as relaxed controls or Fuller phenomenon. All of them are decoded from the analysis of the behavior of solutions of  $\vec{H}_r$  near the switching surface. A corollary of our approach is to deduce that the solutions of  $\vec{H}_r$  are associated to the singularities of the end point mapping  $E : u \rightarrow q(T, q_0, u)$  where  $T$  and  $q_0$  are fixed and  $q(\cdot)$  is the solution of the system at time  $T$ , starting from  $q_0$  and where the control  $u(\cdot)$  is an element of  $L^\infty[0, T]$  with  $|u| = 1$ . In other words, according to the terminology of Bonnard and Chyba (2003), they correspond to singular trajectories if we restrict the control domain to the sphere. From this interpretation we can compute *second-order necessary and sufficient optimality conditions* under generic assumptions. They are implemented in the Cotcot code (see Bonnard, Caillau and Trélat, 2007) which is intensively used in the numerical simulations.

Using this general framework we proceed in Section 3 to a geometric analysis of  $\vec{H}_r$  associated to the two-level dissipative quantum problem. The key property is that the time-minimal control problem has a symmetry of revolution with respect to the  $z$ -axis. This implies the existence of invariant meridian planes corresponding to solutions such that the adjoint component  $p_\theta = 0$  where  $\theta$  is the angle of revolution around the  $z$ -axis. They have an important physical interpretation in the sense that they correspond to extremal solutions with a real laser field. Another property is to observe that the analysis simplifies for specific values of the dissipative parameters such as  $\gamma_- = 0$  and  $\gamma_+ = \Gamma$ . In this case, the distance to the origin  $\rho = |q|$  (i.e. the purity of the system) is not controllable and the problem reduces to a time-minimal control problem on the two-sphere of revolution. A generalized Zermelo navigation problem reduces to a Riemannian problem if the number of inputs is equal to the dimension of the state and if the drift term is zero. Here the associated Riemannian metric on the two-sphere of revolution is  $g = d\phi^2 + \tan^2 \phi d\theta^2$  in spherical coordinates outside the equator  $\phi = \pi/2$ . The optimal curves have been analyzed for this problem in Bonnard et al. (2009). Hence, this is a starting point to make a general analysis using a *continuation method* on the set of parameters.

A detailed analysis of the optimal solutions based on the material of previous sections is presented in the remaining of the article. In Section 4, we classify the optimal syntheses associated to the case where the laser field is real. This corresponds to a time-minimal control problem of a single-input planar system. Section 5 describes the integrable case where  $\gamma_- = 0$  and the generic case  $\gamma_- \neq 0$  is discussed in Section 6 from numerical simulations. An important practical issue corresponding to the robustness with respect to the initial conditions and the dissipative parameters is deduced from our analysis, and discussed in Section 7, from a continuation method.

## 2. Time-minimal control and generalized Zermelo navigation problem

First of all we recall the Pontryagin maximum principle for the time-minimal control problem.

PROPOSITION 1 *Consider the time-minimal control problem for a system of the form:  $\frac{dq}{dt} = f(q(t), u(t))$  where the control domain is a subset  $U$  of  $\mathbb{R}^m$ . If  $(q, u)$  is an optimal solution on  $[0, T]$  then there exists a non-zero adjoint vector  $p(t)$  such that the following equations are satisfied:*

$$\frac{dq}{dt} = \frac{\partial H}{\partial p}, \quad \frac{dp}{dt} = -\frac{\partial H}{\partial q}$$

$$H(q, p, u) = M(q, p),$$

where  $H = \langle p, f(q, u) \rangle$  is the pseudo-Hamiltonian of the system and  $M(q, p) = \max_{v \in U} H(q, p, v)$ . Moreover  $M$  is constant and non negative.

DEFINITION 1 *A generalized Zermelo navigation problem is the time-minimal control problem for a system of the form*

$$\frac{dq}{dt} = F_0(q) + \sum_{i=1}^m u_i F_i(q), \quad |u| \leq 1$$

where  $F_0, F_1, \dots, F_m$  are smooth vector fields on the  $n$ -dimensional manifold  $M$ . We denote by  $g$  the sub-Riemannian metric on  $M$  defined at regular points where  $F_1, \dots, F_m$  form a frame by taking  $F_1, \dots, F_m$  as orthonormal vector fields. For regular points, observe that if  $F_0 = 0$ , we are in the Riemannian case if  $m = n$ , and in the SR-case if  $m < n$ . Moreover if  $m = n$  and  $|F_0|_g < 1$  then it defines a Finsler geometric problem at regular points.

PROPOSITION 2 *Consider a generalized Zermelo navigation problem. Then outside the surface  $\Sigma: H_i = 0, i = 1, \dots, m$ , the optimal solutions are projections on the state space of the solutions of the smooth Hamiltonian vector field  $\vec{H}_r$  of the Hamiltonian  $H_r = H_0 + (\sum_{i=1, m} H_i^2)^{1/2}$  where  $H_i = \langle p, F_i(q) \rangle$  is the Hamiltonian lift of the vector field  $F_i$ .*

*Proof.* We apply the maximum principle for the time-minimal control problem with control bound  $|u| \leq 1$ . The pseudo-Hamiltonian takes the form  $H = H_0 + \sum_i u_i H_i$  and the maximization condition where the control domain is the unit ball gives outside  $\Sigma$ :  $u_i = H_i / \sqrt{\sum_{i=1, m} H_i^2}$  and plugging such control into  $H$  defines the true Hamiltonian  $H_r$ . ■

DEFINITION 2 *The (smooth) solutions  $z$  of  $\vec{H}_r$  are called extremals of order zero and the surface  $\Sigma$  is called the switching surface. In order to be optimal, they have to satisfy  $H_r \geq 0$  and those where  $H_r = 0$  are called abnormal.*

PROPOSITION 3 *Extremal trajectories of order zero correspond to singularities of the end-point mapping  $E^{q_0, T}: u \in L^\infty[0, T] \rightarrow q(T, q_0, u)$  where  $q(\cdot)$  denotes the response to  $u(\cdot)$  with initial condition  $q_0$ , the control domain being restricted to the  $(m - 1)$ -sphere:  $|u| = 1$ .*

This interpretation coming from Riemannian geometry is straightforward but it allows for computing the second-order necessary and sufficient conditions, under generic assumptions for singular extremals using the concept of conjugate point.

### 2.1. Second-order optimality conditions

All the material is borrowed from Bonnard, Caillau and Trélat (2007) and is numerically implemented in the Cotcot code (see the corresponding reference for details). It is based on the theoretical results of Bonnard and Kupka (1993).

#### The concept of conjugate point

Consider a control system of the form:  $\frac{dq}{dt} = f(q, u)$  where the control domain is a  $(m - 1)$ -dimensional manifold  $U$  which can be locally identified with  $\mathbb{R}^{m-1}$ . Using the maximum principle for the time-minimal problem, an optimal control has to satisfy the conditions :  $\frac{\partial H}{\partial u} = 0$ ,  $\frac{\partial^2 H}{\partial u^2} \leq 0$  where  $H$  is the pseudo-Hamiltonian.

Our first assumption is the *strong Legendre-Clebsch condition*:

( $H_1$ ): The Hessian  $\frac{\partial^2 H}{\partial u^2}$  is negative definite along the reference extremal.

From the implicit function theorem, an extremal control can be locally defined as a smooth function  $u(q, p)$  and plugging this function into  $H$  gives the true Hamiltonian  $H_r$ . Setting  $M = \mathbb{R}^n$  and using Hamiltonian formalism, we introduce:

DEFINITION 3 *Let  $z = (q, p)$  be a reference extremal defined on  $[0, T]$ . The variational equation*

$$\frac{d\delta z}{dt} = d\vec{H}_r(z(t))\delta z$$

*is called the Jacobi equation. A Jacobi field is its non trivial solution  $\delta z = (\delta q, \delta p)$ . It is said to be vertical at time  $t$  if  $\delta q(t) = 0$ .*

PROPOSITION 4 *Let  $L_0$  be the fiber  $T_{q_0}^* M$  and let  $L_t = \exp(t\vec{H}_r)(L_0)$  be its image by the local one-parameter group generated by  $\vec{H}_r$ . Then  $L_t$  is a Lagrangian manifold whose tangent space at  $z(t)$  is spanned by the Jacobi fields, vertical at time  $t = 0$ . Moreover, the rank of the restriction to  $L_t$  of the standard projection  $\Pi: (q, p) \rightarrow q$  is at most  $n - 1$ .*

DEFINITION 4 We fix  $q_0 = q(0)$  and we define the exponential mapping:

$$\exp_{q_0} : (p(0), t) \mapsto \Pi(\exp(t\vec{H}_r)(q(0), p(0)))$$

where  $p(0)$  is normalized with  $H_r = \varepsilon$ ,  $\varepsilon = 0, 1$ .

To introduce a relevant concept of conjugate point, one needs further assumptions:

(H<sub>2</sub>): On each subinterval  $[t_0, t_1]$ ,  $0 \leq t_0 < t_1 \leq T$  the image of the derivative of the end-point mapping  $E^{q(t_0), t_1 - t_0}$  is of codimension one for  $u$  restricted to  $[t_0, t_1]$ .

(H<sub>3</sub>): We are in the normal case  $H_r > 0$ .

DEFINITION 5 Let  $z = (q, p)$  be the reference extremal on  $[0, T]$ . Under our assumptions a time  $0 < t_c \leq T$  is called conjugate if the mapping  $\exp_{q_0}$  is not an immersion at  $(p(0), t_c)$  and the point  $q(t_c)$  is said to be conjugate to  $q_0$ . We denote by  $t_{1c}$  the first conjugate time and  $C(q_0)$  the conjugate locus formed by the set of first conjugate points considering all the extremal curves.

We have the following result.

THEOREM 1 Let  $z = (q, p)$  be a reference extremal on  $[0, T]$  satisfying assumptions (H<sub>1</sub>), (H<sub>2</sub>), (H<sub>3</sub>). Then the extremal is optimal in the  $L^\infty$ -norm topology on the set of controls up to the first conjugate time  $t_{1c}$ . Moreover, if  $t \mapsto q(t)$  is one-to-one then it can be embedded into a set  $W$ , image by the exponential mapping of  $N \times [0, T]$ , where  $N$  is a conical neighborhood of  $p(0)$ . For  $T < t_{1c}$ , the reference extremal trajectory is time minimal with respect to all trajectories contained in  $W$ .

In order to get global optimality results, it is necessary to glue together such micro-local sets. For that, we need to introduce the following concepts coming from Riemannian geometry.

DEFINITION 6 Given an extremal trajectory, the first point where it ceases to be optimal is called the cut point and taking all extremals initiating from  $q_0$ , they will form the cut locus  $C_{ut}(q_0)$ . The separating line  $L(q_0)$  is formed by the set of points where two minimizers starting from  $q_0$  intersect.

## 2.2. The case of $m = 2$

In the case of  $m = 2$ , a much more complete analysis can be made using a geometric framework based on the results of Bonnard and Kupka (1993). The main points are the following. Consider a control system of the form:

$$\frac{dq}{dt} = F_0 + u_1 F_1 + u_2 F_2$$

where the control  $u = (u_1, u_2)$  is restricted to the unit circle. An obvious parameterization of the control domain consists in introducing the phase  $\alpha$  such that  $u_1 = \cos \alpha$  and  $u_2 = \sin \alpha$ . We then extend the system with the equation:  $\frac{d\alpha}{dt} = v$  where  $v(\cdot)$  is taken as the new control variable.

From the practical point of view the transformation is meaningful and from the theoretical point of view it corresponds to a Goh transformation relating the original system to a single-input affine system which takes the form

$$\frac{dx}{dt} = F(x) + vG(x)$$

where  $x = (q, \alpha)$  is the extended state space. This transformation allows for applying the theory of Bonnard and Kupka (1993), which is two-fold. First of all, under generic assumptions on Lie brackets of  $F$  and  $G$ , the system can be put into a normal form near the reference singular trajectory for the action of the feedback group in the normal and in the abnormal cases (both cases can be treated similarly using an unfolding). Secondly, this normal form allows to evaluate the end-point mapping in both cases and to define a concept of conjugate point to characterize optimality. In particular, this allows for extending the optimality results in the abnormal case. The computation of conjugate points is implemented in the Cotcot code. Also, the normal form induces a normalization of the Jacobi equation, provided a verticality condition is satisfied at both extremities. More precisely, it takes the form of a self-adjoint differential operator of order  $2(n-1)$  in the normal case and of order  $2(n-2)$  in the abnormal case. A normal form is given by the following proposition:

**PROPOSITION 5** *Any self-adjoint differential operator  $D$  with real coefficients is of even order and can be written*

$$D(x) = (l_0 x^{(r)})^{(r)} + (l_1 x^{(r-1)})^{(r-1)} + \dots + l_r x = 0.$$

*In particular,  $D$  is defined by the  $(r+1)$  functions of time  $l_0, \dots, l_r$ , which play the role of generalized curvatures, corresponding to the concept of conjugate point.*

If the normal form is used as in Bonnard and Kupka (1993) to identify the normal form of the differential operator, in the Cotcot code the concept of conjugate point is intrinsically defined. In this approach, the generalized curvatures are computed using Lie brackets. In particular, we obtain:

**PROPOSITION 6** *Under generic assumptions, the abnormal trajectories of the original system are time-minimizing for the  $L^\infty$ -norm on the set of controls up to a first conjugate time, which can be computed using the Cotcot code.*

### Physical interpretation

The transformed problem established a correspondence between singular trajectories of the extended system, for which  $v \in \mathbb{R}$  and the extremals of order

zero of the original system. Also observe that this problem is not convex since the control lies in a circle. The convexification is obtained by taking the control in the unit ball and can lead to complicated behaviors. For the transformed problem, the time-minimal control problem is well posed if we impose a bound  $|v| \leq M$ . From a practical point of view this condition avoids fast variations of the phase of the laser field.

### 2.3. Shooting method and continuation

The system depends upon three parameters  $(\Gamma, \gamma_+, \gamma_-) \in \Lambda$  such that  $2\Gamma \geq \gamma_+ \geq |\gamma_-|$  and therefore the corresponding Hamiltonian  $H_r$  depends smoothly upon such parameters.

To use the smooth continuation method (see Allgower and Georg, 1990) in the context of optimal control theory, we introduce the following definition:

**DEFINITION 7** *Finding the extremities  $q_0, q_1$ , which solve the shooting equation, means solving the equation*

$$E(x) - q_1 = 0$$

where  $x = (p(0), T) \in S^{n-1} \times \mathbb{R}^+$  and  $E$  is the exponential mapping  $\exp_{q_0}$ .

The following proposition is crucial.

**PROPOSITION 7** *Under our assumptions, the mapping  $E$  is of full rank at  $x = (p(0), T)$  if and only if  $q_1$  is not conjugate to  $q_0$  along the reference extremal.*

This interpretation is essential to compute the adjoint vector by solving the shooting problem and making a *smooth* continuation on the set of parameters. Indeed, one needs to find a homotopy in the set  $\Lambda$  avoiding the conjugate locus. This requires a thorough analysis of the extremal flow for generic values of the parameters in order to get a smooth path when solving the shooting equation. The continuation method will be implemented in Section 7.

## 3. Geometric analysis of Lindblad equation

The main geometric property is a symmetry of revolution with respect to the  $z$ -axis, which is highlighted by the following transformations.

### 3.1. Spherical coordinates

Consider the system (1). We introduce the spherical coordinates

$$x = \rho \sin \phi \cos \theta, \quad y = \rho \sin \phi \sin \theta, \quad z = \rho \cos \phi$$

and we make the following feedback transformations

$$v_1 = u_1 \cos \theta + u_2 \sin \theta, \quad v_2 = -u_1 \sin \theta + u_2 \cos \theta.$$

Then the system becomes

$$\begin{aligned}\dot{\rho} &= \gamma_- \cos \phi - \rho(\gamma_+ \cos^2 \phi + \Gamma \sin^2 \phi) \\ \dot{\phi} &= -\frac{\gamma_- \sin \phi}{\rho} + \frac{\sin(2\phi)}{2}(\gamma_+ - \Gamma) + v_2 \\ \dot{\theta} &= -\cot \phi v_1.\end{aligned}$$

Such a transformation preserves the control bound  $|u| = |v|$  and the Hamiltonian  $H_r$  takes the following form

$$\begin{aligned}H_r &= [\gamma_- \cos \phi - \rho(\gamma_+ \cos^2 \phi + \Gamma \sin^2 \phi)]p_\rho \\ &+ p_\phi[-\frac{\gamma_- \sin \phi}{\rho} + \frac{\sin(2\phi)}{2}(\gamma_+ - \Gamma)] + \sqrt{p_\phi^2 + p_\theta^2 \cot^2 \phi}.\end{aligned}$$

From which we deduce the following proposition:

PROPOSITION 8 *We have:*

1. *The angle  $\theta$  is a cyclic variable and  $p_\theta$  is a first integral (Clairaut relation).*
2. *For  $\gamma_- = 0$ , using the coordinate  $r = \ln \rho$ , the Hamiltonian takes the form:*

$$H_r = -(\gamma_+ \cos^2 \phi + \Gamma \sin^2 \phi)p_r + \frac{\sin(2\phi)}{2}(\gamma_+ - \Gamma)p_\phi + \sqrt{p_\phi^2 + p_\theta^2 \cot^2 \phi}.$$

*Hence,  $r$  is an additional cyclic variable and  $p_r$  is a first integral. The system is thus Liouville integrable.*

The extremals of order zero are solutions of the system:

$$\begin{aligned}\dot{\rho} &= \gamma_- \cos \phi - \rho(\gamma_+ \cos^2 \phi + \Gamma \sin^2 \phi) \\ \dot{\phi} &= -\frac{\gamma_- \sin \phi}{\rho} + \frac{\sin(2\phi)}{2}(\gamma_+ - \Gamma) + \frac{p_\phi}{Q} \\ \dot{\theta} &= \frac{p_\theta \cot^2 \phi}{Q},\end{aligned}$$

while the adjoint system takes the form

$$\begin{aligned}\dot{p}_\rho &= (\gamma_+ \cos^2 \phi + \Gamma \sin^2 \phi)p_\rho - \frac{\gamma_- \sin \phi}{\rho^2}p_\phi \\ \dot{p}_\phi &= [\gamma_- \sin \phi + \rho(\Gamma - \gamma_+) \sin(2\phi)]p_\rho \\ &- [-\frac{1}{\rho} \cos \phi \gamma_- + (\gamma_+ - \Gamma) \cos(2\phi)]p_\phi + \frac{p_\theta^2 \cos \phi}{Q \sin^3 \phi}\end{aligned}$$

where  $p_\theta$  is constant and  $Q = \sqrt{p_\theta^2 \cot^2 \phi + p_\phi^2}$ . It is a complicated system, but it simplifies if  $\gamma_- = 0$  and  $\gamma_+ = \Gamma$ , and we have the following proposition:

PROPOSITION 9 *If  $\gamma_- = 0$  and  $\gamma_+ = \Gamma$ , the coordinate  $\rho$  is not controllable and the time-minimal control problem is equivalent to the almost-Riemannian problem on the two-sphere of revolution:  $g = d\phi^2 + \tan^2 \phi d\theta^2$ .*

*Proof.* The first assertion is clear. Moreover, the evolution of  $(\phi, \theta)$ -variables is given by the Hamiltonian  $\sqrt{p_\theta^2 \cot^2 \phi + p_\phi^2}$  associated to the time-minimal problem for the driftless system on the two-sphere. It is equivalent to the almost-Riemannian problem parameterizing the curves by arc-length, the metric being  $g = d\phi^2 + \tan^2 \phi d\theta^2$ . ■

PROPOSITION 10 *Extremal curves starting from a pole ( $\rho = 1, \phi = 0$  or  $\pi$ ) are such that  $p_\theta = 0$ . They are contained in meridian planes  $\theta = \theta_0$  and up to a  $\theta_0$ -rotation around the  $z$ -axis they are extremals of the 2D-system:*

$$\begin{aligned} \dot{y} &= -\Gamma y - u_1 z \\ \dot{z} &= \gamma_- - \gamma_+ z + u_1 y, |u_1| \leq 1 \end{aligned}$$

where the control is the real part of the laser field.

Another property due to the symmetry of revolution is to concentrate switchings mainly in meridian planes. More precisely we have:

PROPOSITION 11 *Every optimal trajectory is*

1. *Either an extremal trajectory with  $p_\theta = 0$  contained in a meridian plane and time optimal solution of the 2D-system, where  $u = (u_1, 0)$ , while  $\dot{\theta} = -\cot \phi v_1$  along a singular arc,  $v_1$  being any admissible control, and  $\dot{\theta} = 0$  in the non singular case.*
2. *or a subarcs solutions of  $\vec{H}_r$ , where  $p_\theta \neq 0$  with possible connections in the equator plane for which  $\phi = \pi/2$ .*

*Proof.* The first assertion is clear. If  $p_\theta = 0$  then the extremals are defined up to a rotation around the  $z$ -axis by the extremals of the 2D-system, where  $u = (u_1, 0)$ . If  $|u_1| = 1$  then  $\dot{\theta} = 0$  but for a singular arc  $\dot{\theta} = -\cot \phi v_1$  since  $v_1$  is not determined by the condition  $p_\theta = 0$ . The switching surface  $\Sigma$  is defined by:  $p_\theta \cot \phi = p_\phi = 0$ . We cannot connect an extremal with  $p_\theta \neq 0$  to an extremal where  $p_\theta = 0$  since at the connection the adjoint vector has to be continuous. Hence, the only remaining possibility is to connect subarcs of  $\vec{H}_r$  with  $p_\theta \neq 0$  at a point of  $\Sigma$  leading to the conditions  $p_\phi = 0$  and  $\phi = \pi/2$ . ■

The remaining part of this article is devoted to the qualitative analysis of the extremal flow, together with the discussion of the optimality status. According to our previous study, it is splitted into two parts. First of all, we consider the analysis of the time-minimal trajectories for the 2D-single-input system. Such trajectories mainly concentrate the switchings and the maximum principle is crucial for the analysis. Secondly, we consider the analysis of the extremal flow of order zero.

## 4. Time-minimal synthesis of the 2D-case

### 4.1. Generalities

In this section, we consider the time-minimal control problem for the planar single-input system:

$$\begin{aligned}\dot{y} &= -\Gamma y - uz \\ \dot{z} &= \gamma_- - \gamma_+ z + uy, |u| \leq 1.\end{aligned}$$

The initial state is the pure state  $(y, z) = (0, 1)$  on the  $z$ -axis. The time-minimal control is computed as a closed loop function  $u(q)$ . The system is written as  $\frac{dq}{dt} = F(q) + uG(q)$  and, according to the maximum principle, an optimal control is the concatenation of bang arcs  $\sigma_+$  and  $\sigma_-$  corresponding to  $u = +1$  and  $u = -1$  and singular arcs  $\sigma_s$  located on the set:  $S = \{q; \det(G, [F, G]) = 0\}$  provided the singular control satisfies the bound  $|u| \leq 1$ . Another important set when computing the optimality synthesis is the collinear set:  $C = \{q; \det(F, G) = 0\}$ .

The time-minimal synthesis can be computed according to geometric optimal control theory using the following two steps:

#### Step 1

Classify all the optimal syntheses encountered in the problem on a small neighborhood of a given point of the unit ball (in the analytic framework this depends upon the configuration of Lie brackets of  $F$  and  $G$ ).

#### Step 2

Glue together all the local results using topological analysis and computations of the switching rules in order to get the global result.

The first step can be easily performed using Lie brackets computations and the standard literature on the subject (see Bonnard and Chyba, 2003, and Boscain and Piccoli, 2004). The second step is based on theoretical and numerical simulations to determine the switching sequences. In what follows, we present the geometric framework to perform such computations.

### 4.2. The switching function

Instead of using the adjoint equation to determine the switching sequences, we introduce the following coordinate invariant point of view. Assume  $0, t$  be two consecutive switching times on an arc  $\sigma_+$  or  $\sigma_-$  where the control is  $u = \varepsilon = \pm 1$ . We must have:

$$p(0)G(q(0)) = p(t)G(q(t)) = 0.$$

We denote by  $v(\cdot)$  the solution of the variational equation such that  $v(t) = G(q(t))$ , where this equation is integrated backwards from time  $t$  to time  $0$ . By

construction,  $p(0)v(0) = 0$  and we deduce that at time 0,  $p(0)$  is orthogonal to  $G(q(0))$  and to  $v(0)$ . Therefore,  $v(0)$  and  $G(q(0))$  are collinear;  $\Theta(t)$  is defined as the angle between  $G(q(0))$  and  $v(0)$  measured counterclockwise. One deduces that switching occurs when  $\Theta(t) = 0 \text{ } [\pi]$ . This can be tested using

$$\det(G(q_0), v(0)) = 0. \quad (3)$$

We have, by definition

$$v(0) = e^{-t\text{ad}(F+\varepsilon G)}G(q(t)),$$

and in the analytic case, the ad-formula gives :

$$v(0) = \sum_{n \geq 0} \frac{(-t)^n}{n!} \text{ad}^n(F + \varepsilon G)G(q(t)).$$

Here, to make the computation explicit, we take advantage of the fact that we can lift our bilinear system into an invariant system onto the semi-direct product Lie group  $GL(2, \mathbb{R}) \times_S \mathbb{R}^2$  identified with the set of matrices of  $GL(3, \mathbb{R})$ :

$$\begin{pmatrix} 1 & 0 \\ g & v \end{pmatrix}, \quad g \in GL(2, \mathbb{R}), \quad v \in \mathbb{R}^2,$$

acting on the subspace of vectors in  $\mathbb{R}^3$ :  $\begin{pmatrix} 1 \\ q \end{pmatrix}$ .

Lie bracket computations are defined as follows. We set:

$$F(q) = Aq + a, \quad G(q) = Bq,$$

and  $F, G$  are identified to  $(A, a), (B, 0)$  in the Lie algebra  $\underline{gl}(2, \mathbb{R}) \times \mathbb{R}^2$ . The Lie bracket computations on the semi-direct product Lie algebra are defined by:

$$[(A', a'), (B', b')] = ([A', B'], A'b' - B'a').$$

We now compute  $\exp[-t\text{ad}(F + \varepsilon G)]$ . The first step consists in determining  $\exp[-t\text{ad}(A + \varepsilon B)]$  which amounts to computing  $\text{ad}(A + \varepsilon B)$ .

#### Case of $\gamma_- = 0$

We set  $F(q) = Aq$  and  $G(q) = Bq$ . We write  $\underline{gl}(2, \mathbb{R}) = c \oplus \underline{sl}(2, \mathbb{R})$  where  $c$  is the center. We choose the following basis of  $\underline{sl}(2, \mathbb{R})$ :

$$B = \begin{pmatrix} 0 & -1 \\ 1 & 0 \end{pmatrix}, \quad C = \begin{pmatrix} 0 & 1 \\ 1 & 0 \end{pmatrix} \quad \text{and} \quad D = \begin{pmatrix} 1 & 0 \\ 0 & -1 \end{pmatrix}.$$

The matrix  $A$  is decomposed into:

$$A = \begin{pmatrix} -\Gamma & 0 \\ 0 & -\gamma_+ \end{pmatrix} = \begin{pmatrix} \lambda & 0 \\ 0 & \lambda \end{pmatrix} + \begin{pmatrix} s & 0 \\ 0 & -s \end{pmatrix}$$

and hence  $\lambda = -(\Gamma + \gamma_+)/2$  and  $s = (\gamma_+ - \Gamma)/2$ . In the basis  $(B, C, D)$ ,  $\text{ad}(A + \varepsilon B)$  is represented by the matrix:

$$\begin{pmatrix} 0 & -2s & 0 \\ -2s & 0 & 2\varepsilon \\ 0 & -2\varepsilon & 0 \end{pmatrix}.$$

The characteristic polynomial is  $P(\lambda) = -\lambda(\lambda^2 + 4(\varepsilon^2 - s^2))$  and the eigenvalues are  $\lambda = 0$  and  $\lambda_i = \pm 2\sqrt{s^2 - \varepsilon^2}$ ,  $i = 1, 2$ ;  $\lambda_1$  and  $\lambda_2$  are distinct and real if  $|\gamma_+ - \Gamma| > 2$  and we note  $\lambda_1 = 2\sqrt{s^2 - \varepsilon^2}$ ,  $\lambda_2 = -\lambda_1$ ;  $\lambda_1$  and  $\lambda_2$  are distinct and imaginary if  $|\gamma_+ - \Gamma| < 2$  and we note  $\lambda_1 = 2i\sqrt{\varepsilon^2 - s^2}$ ,  $\lambda_2 = -\lambda_1$ . To compute  $e^{-\text{tad}(A+\varepsilon B)}$ , we must distinguish two cases:

**Real case:** In the basis  $B, C, D$ , the eigenvectors corresponding to  $\{0, \lambda_1, \lambda_2\}$  are, respectively:  $v_0 = {}^t(\varepsilon, 0, s)$ ,  $v_1 = {}^t(2s, -\lambda_1, 2\varepsilon)$  and  $v_2 = {}^t(2s, -\lambda_2, 2\varepsilon)$ . Therefore, in this eigenvector basis,  $\exp[-\text{tad}(A + \varepsilon B)]$  is the diagonal matrix:  $\text{diag}(1, e^{-\lambda_1 t}, e^{-\lambda_2 t})$ . To compute  $\exp[-\text{tad}(A + \varepsilon B)]B$ , we use the decomposition

$$B = \alpha v_0 + \beta v_1 + \beta v_2,$$

with:

$$\alpha = \frac{\varepsilon}{\varepsilon^2 - s^2}, \quad \beta = \frac{s}{4(s^2 - \varepsilon^2)}.$$

Hence, one gets:

$$e^{-\text{tad}(A+\varepsilon B)}B = \alpha v_0 + \beta e^{-\lambda_1 t} v_1 + \beta e^{-\lambda_2 t} v_2.$$

To test the collinearity at  $q_0$ , we compute

$$\det(B(q_0), e^{-\text{tad}(A+\varepsilon B)}B(q_0)) = 0$$

where the determinant is equal to

$$(z_0^2 - y_0^2)(\alpha s + 2\varepsilon(\beta e^{-\lambda_1 t} + \beta e^{-\lambda_2 t})) + 2y_0 z_0(\lambda_1 \beta e^{-\lambda_1 t} + \lambda_2 \beta e^{-\lambda_2 t}).$$

**Imaginary case:** In this case, we note  $\lambda_1 = i\theta$  the eigenvalue associated to the eigenvector  ${}^t(2s, -i\theta, 2\varepsilon)$ . We consider the real part  $v_1 = {}^t(2s, 0, 2\varepsilon)$  and the imaginary part  $v_2 = {}^t(0, -\theta, 0)$ . In the basis  $v_0 = {}^t(\varepsilon, 0, s)$ ,  $v_1, v_2$ ,  $\text{ad}(A + \varepsilon B)$  takes the normal form:

$$\text{diag}(0, \begin{pmatrix} 0 & \theta \\ -\theta & 0 \end{pmatrix}).$$

Computing as before, we obtain that the determinant is given by:

$$(z_0^2 - y_0^2)(\alpha s + 4\varepsilon\beta \cos(\theta t)) + 4\beta\theta \sin(\theta t)y_0 z_0.$$

Hence we deduce the following switching rules:

PROPOSITION 12 *Assume  $\gamma_- = 0$  and that a switching occurs at times  $0, t$  along an arc  $\sigma_\varepsilon$  initiating from  $(y_0, z_0)$ . Then*

1. *if  $|\gamma_+ - \Gamma| > 2$ , we must have:*

$$(z_0^2 - y_0^2)(\alpha s + 4\varepsilon\beta \cosh(\lambda_1 t)) - 4y_0 z_0 \beta \lambda_1 \sinh(\lambda_1 t) = 0$$

where  $\alpha = \frac{\varepsilon}{\varepsilon^2 - s^2}$ ,  $\beta = \frac{s}{4(s^2 - \varepsilon^2)}$  and  $\lambda_1 = 2\sqrt{s^2 - \varepsilon^2}$ ;

in particular, if  $(y_0, z_0) = (0, 1)$  there is no switching for  $t > 0$ ;

2. *if  $|\gamma_+ - \Gamma| < 2$ , we must have:*

$$(z_0^2 - y_0^2)(\alpha s + 4\varepsilon\beta \cos(\theta t)) + 4\beta\theta \sin(\theta t)y_0 z_0 = 0$$

where  $\theta = 2\sqrt{\varepsilon^2 - s^2}$ ,  $\alpha = \frac{\varepsilon}{\varepsilon^2 - s^2}$ ,  $\beta = \frac{s}{4(s^2 - \varepsilon^2)}$ ;

in particular, if  $(y_0, z_0) = (0, 1)$  switching occurs periodically with the period  $2\pi/\theta$ .

### Case of $\gamma_- \neq 0$

The computations are more complex, but this case is similar. The vector field  $F + \varepsilon G$  is an affine vector field and to simplify the computations it is transformed into the linear vector field  $A + \varepsilon B$  by making the following translation in the  $\mathbb{R}^2$  space:  $Y = y + \tilde{y}$ ,  $Z = z + \tilde{z}$  with  $\tilde{y} = \varepsilon\gamma_- / (\Gamma\gamma_+ + \varepsilon^2)$  and  $\tilde{z} = -\Gamma\gamma_- / (\Gamma\gamma_+ + \varepsilon^2)$ .  $G$  is transformed into the affine vector  $Bq + w$  where  $w$  is the vector  $(w_1, w_2)$  with  $w_1 = -\Gamma\gamma_- / (\Gamma\gamma_+ + \varepsilon^2)$  and  $w_2 = -\varepsilon\gamma_- / (\Gamma\gamma_+ + \varepsilon^2)$ . The vector field  $\text{ad}(F + \varepsilon G)$  acts on the vector space  $\mathfrak{gl}(2, \mathbb{R}) \oplus \mathbb{R}^2$  and the action on the space  $\mathfrak{gl}(2, \mathbb{R})$  has been previously computed. According to the definition of the Lie bracket, the action on the  $\mathbb{R}^2$  space is simply the action of the linear operator  $A + \varepsilon B$ . The characteristic polynomial is  $P = \lambda^2 + (\Gamma + \gamma_+)\lambda + (\Gamma\gamma_+ + \varepsilon^2)$ . We must distinguish two cases:

**Real case:** If  $|\Gamma - \gamma_+| > 2$ , we have two real eigenvalues

$$\sigma_1 = \frac{-(\Gamma + \gamma_+) + 2\sqrt{s^2 - \varepsilon^2}}{2}, \quad \sigma_2 = \frac{-(\Gamma + \gamma_+) - 2\sqrt{s^2 - \varepsilon^2}}{2}$$

with corresponding eigenvectors  $f_1$  and  $f_2$ . Writing the vector  $w$  as  $\delta_1 f_1 + \delta_2 f_2$ , one gets, using the previous computations,

$$e^{-\text{tad}(F + \varepsilon G)} G = \alpha v_0 + \beta e^{-\lambda_1 t} v_1 + \gamma e^{-\lambda_2 t} v_2 + \delta_1 e^{-\sigma_1 t} f_1 + \delta_2 e^{-\sigma_2 t} f_2.$$

**Complex case:** If  $|\Gamma - \gamma_+| < 2$ , we have two complex eigenvalues  $-(\Gamma + \gamma_+) \pm 2i\sqrt{\varepsilon^2 - s^2}/2$ . The computation of the exponential of the operator is similar using a real Jordan normal form.

### 4.3. The classification of the optimal syntheses

In order to determine a 2D-time optimal synthesis, we must compute:

- The switching locus  $\Sigma_1$  of optimal trajectories.
- The cut locus which is formed by the set of points where a minimizer ceases to be optimal.

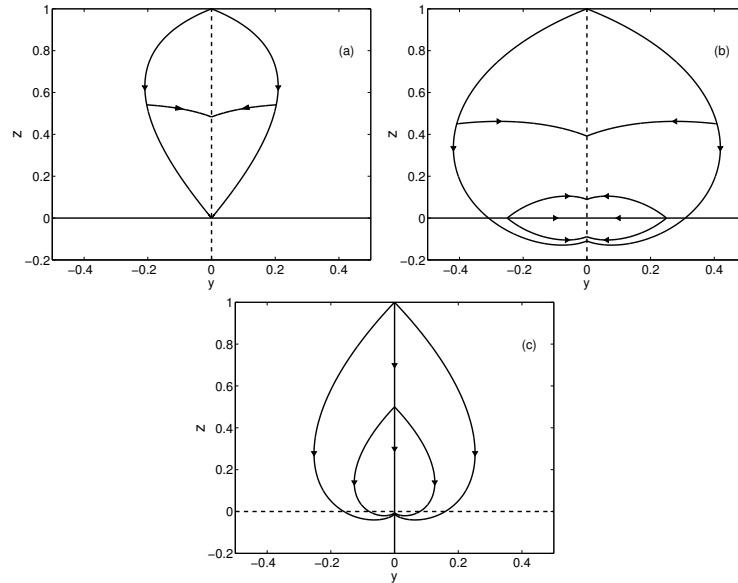


Figure 1. Optimal syntheses for (a) ( $\Gamma = 3, \gamma_+ = 0.6, \gamma_- = 0$ ), (b) ( $\Gamma = 0.8, \gamma_+ = 0.6, \gamma_- = 0$ ) and (c) ( $\Gamma = 1.1, \gamma_+ = 1.6, \gamma_- = 0$ ). Solid and dashed vertical and horizontal lines correspond, respectively, to fast and slow singular lines. The set  $C$  is restricted to the origin.

We have represented in Figs. 1 and 2 the optimal syntheses for  $\gamma_- = 0$  and  $\gamma_- \neq 0$ . They are computed for the given values of the parameters. The classification is complete up to some *microscopic* switching effects localized near the singular point of  $F + \varepsilon G$ . Observe the symmetry with respect to the  $z$ -axis, due to the symmetry of revolution of the whole system and the various bifurcation schemes. Observe also the complexity of the case  $\gamma_- \neq 0$ . Moreover, it cannot be deduced from the case  $\gamma_- = 0$ , for which the collinear set  $C$  shrinks to 0, which concentrates all the singularities. We point out that the case  $\gamma_- = 0$  is not relevant from the generic point of view.

### 5. The bi-input case

We now proceed to the analysis of the time-minimal control problem, when the initial state  $q_0 = {}^t(x_0, y_0, z_0)$  is not at the poles, by making the synthesis from the Hamiltonian  $H_r$  with  $p_\theta$  non zero. From the previous section, we observe that switchings can occur in meridian planes. To complete the analysis, one must consider the possible switchings of optimal trajectories near the equator  $\phi = \pi/2$ .

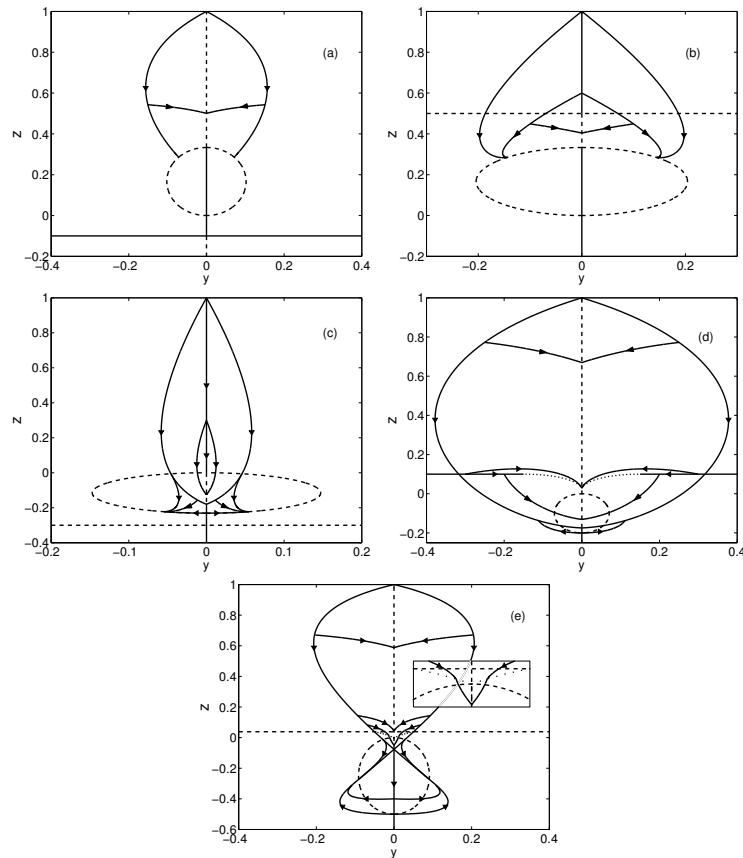


Figure 2. Optimal syntheses for (a) ( $\Gamma = 4$ ,  $\gamma_+ = 1.5$ ,  $\gamma_- = 0.5$ ), (b) ( $\Gamma = 2$ ,  $\gamma_+ = 3$ ,  $\gamma_- = 1$ ), (c) ( $\Gamma = 4$ ,  $\gamma_+ = 6.5$ ,  $\gamma_- = -1.5$ ), (d) ( $\Gamma = 1$ ,  $\gamma_+ = 0.5$ ,  $\gamma_- = -0.1$ ) and (e) ( $\Gamma = 3$ ,  $\gamma_+ = 0.4$ ,  $\gamma_- = -0.2$ ). Solid and dashed vertical and horizontal lines correspond, respectively, to fast and slow singular lines. The set  $C$  is represented in dashed lines. The switching locus is plotted in dotted lines in (d) and (e). In (d), only the admissible singular horizontal line is represented in solid line. In (e), the small insert is a zoom of the optimal synthesis near the origin.

### 5.1. Regularity analysis near $\phi = \pi/2$

The first step consists in constructing a normal form. Taking the system in spherical coordinates and setting  $\psi = \pi/2 - \phi$ , we consider the approximation:

$$\begin{aligned}\dot{\rho} &= \gamma_- \psi - \rho(\Gamma + (\gamma_+ - \Gamma)\psi^2) \\ \dot{\psi} &= \frac{\gamma_-}{\rho} \left(1 - \frac{\psi^2}{2}\right) - \psi(\gamma_+ - \Gamma) - v_2 \\ \dot{\theta} &= -\psi v_1\end{aligned}$$

with the corresponding Hamiltonian:

$$\begin{aligned}H_r &= p_\rho[\gamma_- \psi - \rho(\Gamma + (\gamma_+ - \Gamma)\psi^2)] + p_\psi \left(\frac{\gamma_-}{\rho} \left(1 - \frac{\psi^2}{2}\right)\right) \\ &\quad - \psi(\gamma_+ - \Gamma) + \sqrt{p_\psi^2 + p_\theta^2 \psi^2}.\end{aligned}$$

**PROPOSITION 13** *Near  $\Sigma : \psi = 0, p_\psi = 0$ , we have two distinct cases for optimal trajectories:*

- *If  $\gamma_- = 0$ , for the 2D-system, the line  $\psi = 0$  is a singular trajectory with admissible zero control if  $\gamma_+ - \Gamma \neq 0$ . It is slow if  $(\gamma_+ - \Gamma) > 0$  and fast if  $(\gamma_+ - \Gamma) < 0$ . Hence, for this system, we get only optimal trajectories through the switching surface  $\Sigma$  in the case  $(\gamma_+ - \Gamma) < 0$ , where  $\psi$  is of order  $t$  and  $p_\psi$  of order  $t^2$ . They are the only non-smooth optimal trajectories passing through  $\Sigma$ .*
- *If  $\gamma_- \neq 0$ , for the 2D-system, the set  $\psi = p_\psi = 0$  becomes a set of ordinary switching points where  $\psi$  and  $p_\psi$  are of order  $t$ . Moreover, connections for extremals of  $\vec{H}_r$  with  $p_\theta \neq 0$  are eventually possible, depending upon the set of parameters and initial conditions.*

### 5.2. The integrable case $\gamma_- = 0$

We now present the analysis for the case  $\gamma_- = 0$ . This is not a stable case, as shown, for instance, by the previous section. This case has, however, a double mathematical interest. First of all, a complete mathematical analysis can be made using a continuation method from the so-called *Grushin almost Riemannian metric on the two-sphere of revolution*:  $g = d\phi^2 + \tan^2 \phi d\theta^2$ . Making this continuation, we observe a bifurcation when  $|\gamma_+ - \Gamma| = 2$  and the existence of a barrier phenomenon for the  $\phi$ -variable. This phenomenon persists in the general case of  $\gamma_- \neq 0$ .

#### The Grushin case on the two-sphere of revolution

If  $g = d\phi^2 + \tan^2 \phi d\theta^2$ , then we have an almost-Riemannian metric on the two-sphere of revolution, with a singularity at the equator  $\phi = \pi/2$ , which is

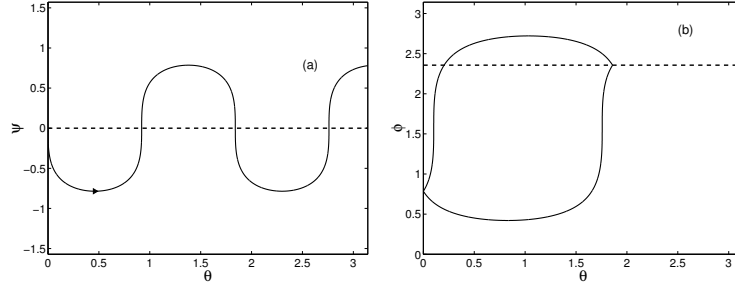


Figure 3. (a) Periodic oscillation of the  $\psi$ -variable as a function of  $\theta$ . (b) Two extremal curves with the same length intersect on the antipodal parallel depicted in dashed lines.

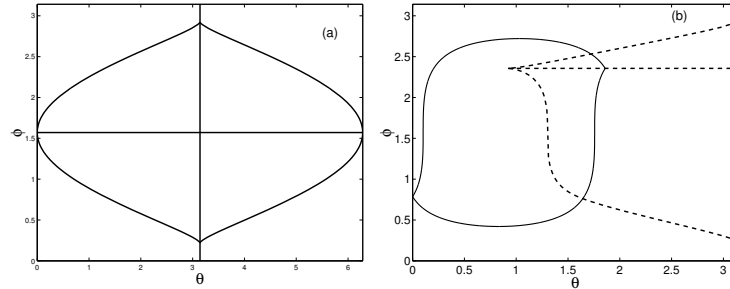


Figure 4. (a) Conjugate locus for an initial condition on the equator. (b) Conjugate locus for an initial condition not on the equator.

reflexionally symmetric with respect to the equator. For such a metric, the extremal curves have a simple structure and we can determine the conjugate and cut loci of any point.

**Extremal curves:** If  $p_\theta = 0$ , we get the meridian circles and for  $p_\theta \neq 0$ ,  $\psi = \pi/2 - \phi$  oscillates periodically between  $\psi_{max}$  and  $\psi_{min}$ . Also, due to a central symmetry, two curves starting from  $(\phi(0), 0)$  intersect on the antipodal parallel with the same length.

**Conjugate and cut loci:** We have three cases.

- Pole: The conjugate and cut loci of a pole is the antipodal point.
- Equator: The closure of the cut is the whole equator, while the conjugate locus is represented in Fig. 4a.
- Point not on a pole, nor on the equator: The cut locus is a single branch on the antipodal parallel while the conjugate locus is diffeomorphic to a standard astroid (see Fig. 4b).

This gives the analysis for the case of  $\gamma_- = 0, \gamma_+ = \Gamma$ , since the coordinate  $r = \ln \rho$  is not controllable.

Making a small deformation on  $\gamma_+$  and  $\Gamma$  and fixing  $p_r$ , we observe that the projections of the extremal curves on the two-sphere have the same shape and the whole Hamiltonian  $H_r$  remains invariant for the transformation  $(\phi, p_\phi) \mapsto (\pi - \phi, -p_\phi)$ . As a consequence, we have:

**LEMMA 1** *For  $\gamma_- = 0$  and  $|\gamma_+ - \Gamma| \simeq 0$ , we have for fixed  $(p_\theta, p_r)$ ,  $p_\theta \neq 0$  a family of two distinct extremal curves  $q^+(t)$  and  $q^-(t)$  starting from the same point and intersecting with the same time  $T/2$  at a point such that  $\phi(T/2) = \pi - \phi(0)$ ,  $T$  being the period of the angular variable  $\phi$ .*

It can be easily seen that this property persists up to  $|\gamma_+ - \Gamma| = 2$ . More precisely, if we consider the system restricted to the two-sphere:

$$\begin{aligned} \dot{\phi} &= \frac{\sin(2\phi)}{2}(\gamma_+ - \Gamma) + v_2 \\ \dot{\theta} &= -\cot \phi v_1 \end{aligned} \tag{4}$$

we have the following proposition:

**PROPOSITION 14** *The time-minimal control problem for system (4) on the two-sphere defines a Zermelo navigation problem, reflexionally symmetric with respect to the equator, for the metric  $g = d\phi^2 + \tan^2 \phi d\theta^2$ , which is singular at the equator. The current in the north-hemisphere is maximal for  $\phi = \pi/4$  and can be compensated by feedback on the whole sphere if  $|\gamma_+ - \Gamma| < 2$ . In this case, this defines a Finsler geometry on the whole sphere minus the equator.*

This property allows for analyzing the case of  $|\gamma_+ - \Gamma| < 2$ .

**Case of  $|\gamma_+ - \Gamma| < 2$**

In this case, the extremal curves share similar properties with respect to the Grushin model. The projection on the two-sphere is represented in Fig. 5a, while the evolution of the additional variable  $r$  is represented in Fig. 5b. Concerning the optimality status, the extremal curves have conjugate points. Due to the symmetry property  $(\phi, p_\phi) \mapsto (\pi - \phi, -p_\phi)$ , extremal curves starting from  $\phi(0)$ , with  $p_r$  fixed, whose projection intersects on the antipodal point  $\pi - \phi(0)$  on the two-sphere, intersects also on the whole space from Lemma 1. For fixed  $p_r$ , we represent the projection of the conjugate and cut loci on the two-sphere compared with the case of  $\gamma_+ = \Gamma$  in Fig. 6.

**Case of  $|\gamma_+ - \Gamma| > 2$**

In this case, a new behavior is observed, since the current cannot be compensated near  $\phi = \pi/4$ . Indeed, upon taking  $v_1 = 0$  in (4), the equation in a meridian

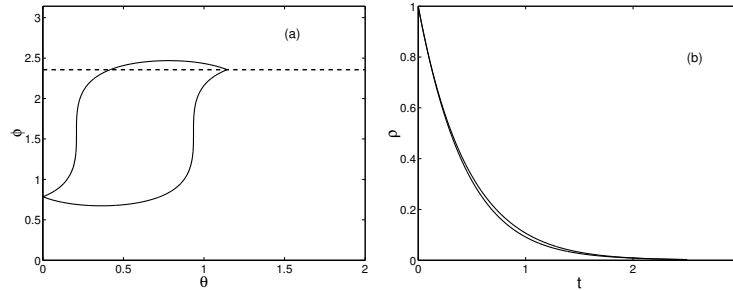


Figure 5. Extremal trajectories for  $\Gamma = 2.5$ ,  $\gamma_+ = 2$  and  $\gamma_- = 0$ . The dashed line represents the antipodal parallel.

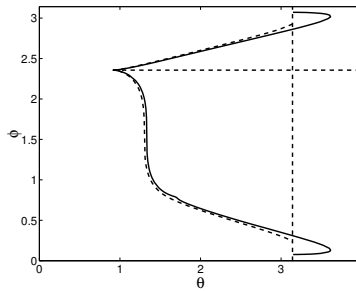


Figure 6. Projection of conjugate locus in solid line for  $p_\rho = 0.5$  and  $p_\theta = 2$ . Dissipative parameters are taken to be  $\Gamma = 2.5$ ,  $\gamma_+ = 2$  and  $\gamma_- = 0$ . The conjugate locus of the Grushin model corresponding to  $\gamma_+ = \Gamma = 2$  is represented by dashed lines. The horizontal dashed line indicates the position of the cut locus for the Grushin model.

plane becomes:

$$\dot{\phi} = \frac{\sin(2\phi)(\gamma_+ - \Gamma)}{2} + v_2.$$

We have a singularity if  $(\gamma_+ - \Gamma)^2 \sin^2(2\phi)/4 = 1$ . For the whole system, this gives the following proposition:

PROPOSITION 15 *If  $|\Gamma - \gamma_+| \geq 2$  then we have extremal trajectories such that  $\dot{\phi} \rightarrow 0$ ,  $\dot{\theta} \rightarrow 0$  and  $|p_\phi| \rightarrow +\infty$  when  $t \rightarrow +\infty$ .*

Such extremals coexist with extremals located near the equator, whose behavior is similar to those corresponding to  $|\gamma_+ - \Gamma| < 2$ , since the current can be compensated by feedback near the equator (see Fig. 7).

**Optimality status:** One checks that extremals such that  $\phi$  is not periodic have no conjugate point, while those, where  $\phi$  is periodic, are as before.

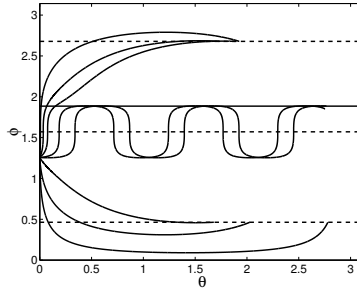


Figure 7. Extremal trajectories for  $\Gamma = 4.5$ ,  $\gamma_+ = 2$  and  $\gamma_- = 0$ . Dashed lines represent the equator and the locus of the fixed points of the dynamics. The solid line corresponds to the antipodal parallel. Numerical values of the parameters are taken to be  $\phi(0) = 2\pi/5$ ,  $p_\theta = 8$  and  $p_\rho(0) = 0.25$ . The different initial values of  $p_\phi$  are  $-50, -10, 0, 2.637, 3, 5, 10$  and  $50$ .

### 6. The generic case

The previous analysis when  $\gamma_- = 0$  is not sufficient to analyze the generic case of  $\gamma_- \neq 0$ . This was already observed in Section 4, where we have classified the time-minimal syntheses in meridian planes. It can also be conjectured from the analysis of Section 5, where we have a family of extremal curves such that the evolution of  $\phi$  is periodic, that this property should disappear by perturbation. From the previous analysis, we observe a new family of trajectories such that the level set  $H_r = 1$  is not compact, since  $|p_\phi| \rightarrow +\infty$ . These trajectories are classified using the asymptotic behaviors of the  $\phi$  variable.

In the generic case of  $\gamma_- \neq 0$ , we made numerical simulations, integrating the extremal flow and testing the existence of conjugate points. We observe two distinct behaviors.

**PROPOSITION 16** *In the case denoted (a), we have extremal curves such that  $|p_\phi| \rightarrow +\infty$  when  $t \rightarrow +\infty$  and the asymptotic stationary points  $(\rho_f, \phi_f, \theta_f)$  of the dynamics depend upon the dissipative parameters. Such curves have no conjugate point.*

**PROPOSITION 17** *In the case denoted (b),  $p_\phi$  oscillates periodically between  $\pm\infty$ ,  $\phi \rightarrow 0$  or  $\pi$  and  $\rho \rightarrow \gamma_-/|\gamma_+|$  when  $t \rightarrow +\infty$ . Such trajectories have conjugate points.*

We have numerically observed that if  $|\Gamma - \gamma_+| > 2$ , then only case (a) is encountered, whereas if  $|\Gamma - \gamma_+| < 2$ , the extremals are described by the case (b). Both behaviors are compared in Fig. 8, making a continuation on the set of parameters. Fig. 9 displays the different behaviors of the  $p_\phi$  variable with the corresponding control  $(v_1, v_2)$ . Note that when  $p_\phi$  oscillates, we have an additional

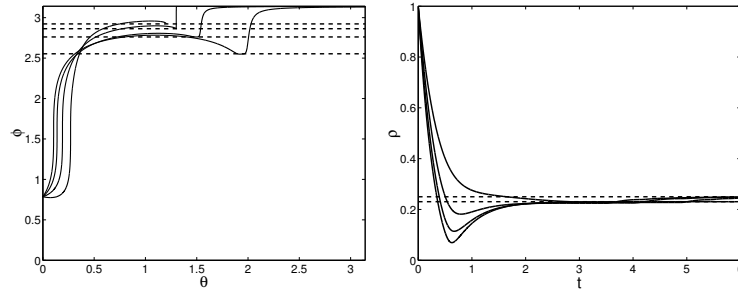


Figure 8. Extremal trajectories for  $\Gamma \in \{1.5, 2.5, 3.5, 4.5\}$ ,  $\gamma_+ = 2$ ,  $\gamma_- = -0.5$ ,  $\phi(0) = \pi/4$ ,  $p_r(0) = 0.1$  and  $p_\theta = 2$ . Dashed lines represent the asymptotic fixed point of the dynamics for the  $\phi$  and  $\rho$  variables (see Propositions 16 and 17).

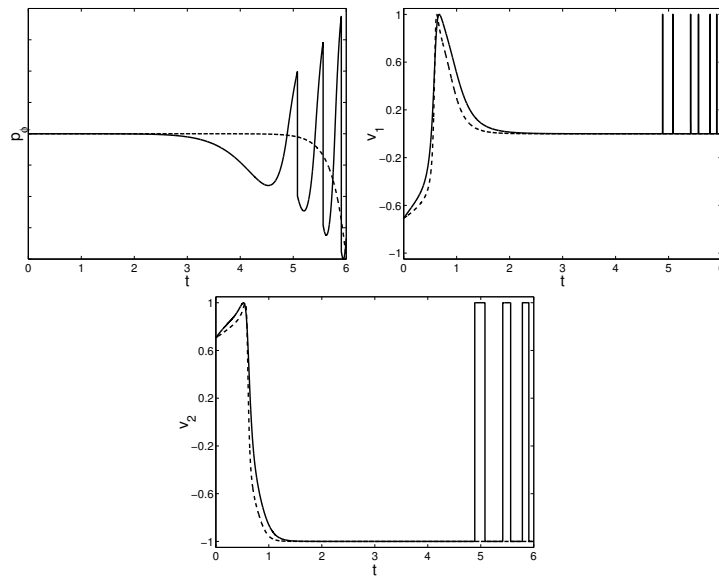


Figure 9. Evolution of the adjoint coordinate  $p_\phi$  and of the control fields  $v_1$  and  $v_2$  as a function of  $t$  for  $\Gamma \in \{3.5, 4.5\}$ ,  $\gamma_+ = 2$ ,  $\gamma_- = -0.5$ ,  $\phi(0) = \pi/4$ ,  $p_r(0) = 0.1$  and  $p_\theta = 2$ . The plots associated to  $\Gamma = 3.5$  (respectively  $\Gamma = 4.5$ ) are represented in solid lines (respectively dashed lines).

singularity, since  $v_1 = p_\phi / \sqrt{p_\phi^2 + p_\theta^2 \cot^2 \phi}$  and  $v_2 = p_\theta \cot \phi / \sqrt{p_\phi^2 + p_\theta^2 \cot^2 \phi}$  while  $\phi \rightarrow 0$  or  $\pi$  and  $\cot \phi \rightarrow \infty$ . Numerical simulations show that  $|p_\phi|$  dominates  $\cot \phi$  at infinity.

An important remark is the existence of conjugate points in the second case, which prevents the existence of optimal trajectories with a Fuller phenomenon due to the oscillatory behavior of  $p_\phi$ . We deduce that an important theoretical study has to be made to classify the extremal trajectories near a compactification at the infinity of the switching surface  $\Sigma$ .

## 7. The continuation method

To complete the analysis, we implement the continuation method. In our problem, the essential parameters associated to the homotopy are either  $\Gamma - \gamma_+$  or  $\gamma_-$ . One particular objective of this section is to understand the role of the bifurcations of extremal trajectories on the continuation. We recall that the bifurcations arise for  $|\Gamma - \gamma_+| = 2$  and  $\gamma_- = 0$ . A discrete continuation method is sufficient in our case. The Newton routine, which allows for determining at each step of the continuation method the new adjoint vector, has been implemented in *MatLab*. We have solved different three-dimensional homotopy problems with a final condition on the radial coordinate or on its adjoint vector when the final radial coordinate is not fixed.

The structure of the algorithm can be summarized as follows. At each step of an iteration, we modify by a certain amount the continuation parameter ( $\Gamma - \gamma_+$ ) or  $\gamma_-$ . Starting from the initial adjoint vectors and the final time of the preceding iteration, we determine by a Newton routine the new initial adjoint vectors and the new final time which allow for reaching a fixed target state from the same initial state.

### 7.1. The case of a free final radial coordinate

In this case, the final purity  $\rho_f$  is not fixed at the final time  $t_f$ . We therefore add the transversality condition  $p_{\rho_f} = 0$  at  $t = t_f$  in the shooting equation. The target state is denoted by  $(p_{\rho_f} = 0, \phi_f, \theta_f)$  and at each step of iteration, we adjust  $p_{\rho_f}(0)$ ,  $p_\phi(0)$  and  $t_f$  to reach the target state. We consider the homotopy method with respect to the parameters  $\Gamma$  and  $\gamma_-$ . We have obtained very good results, with no problem of convergence, when the duration of the control is sufficiently small. We have found that the maximum variation of the parameters to ensure the convergence of the method can be very large, of the order of  $10^{-2}$ . We have observed that the bifurcations in  $|\Gamma - \gamma_+| = 2$  and  $\gamma_- = 0$  play no role in the variation of the different parameters as long as the target state belongs to the accessible set. We have chosen small control durations to avoid such problems. An example of modifications of the accessible set is given in Fig. 8. One clearly sees that this set is smaller for extremals described by the case (b) than for the ones of case (a).

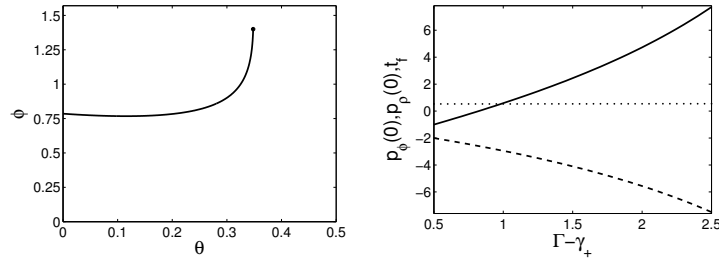


Figure 10. Continuation with respect to  $\Gamma - \gamma_+$ . The parameters of the initial point are  $\Gamma = 2.5$ ,  $\gamma_+ = 2$ ,  $\gamma_- = -0.5$ ,  $\phi(0) = \pi/4$ ,  $p_\rho(0) = -2$ ,  $p_\theta = 8$  and  $p_\phi(0) = -1$ . The initial time is  $t_f = 0.5287$ . The target state corresponds to  $\phi_f = 1.4004$ ,  $\theta_f = 0.3481$  and  $p_{\rho f} = 0$ . The first figure represents the extremal trajectory solution of the continuation problem for  $\Gamma = 4.5$  and  $\gamma_+ = 2$ ;  $p_\phi(0)$ ,  $p_\rho(0)$  and  $t_f$  are, respectively, plotted in solid, dashed and dotted lines.

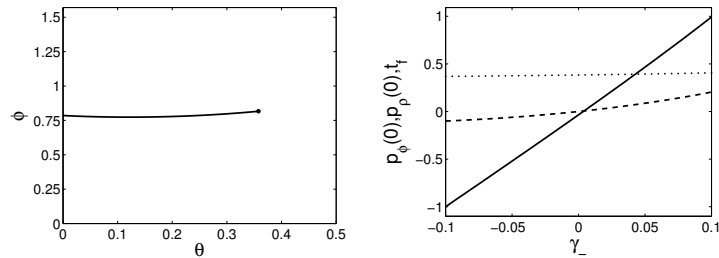


Figure 11. Continuation with respect to  $\gamma_-$ . The parameters of the initial point are  $\Gamma = 2.5$ ,  $\gamma_+ = 2$ ,  $\gamma_- = -0.1$ ,  $\phi(0) = \pi/4$ ,  $p_\rho(0) = -0.1$ ,  $p_\theta = 8$  and  $p_\phi(0) = -1$ . The initial time is  $t_f = 0.3683$ . The target state corresponds to  $\phi_f = 0.816474$ ,  $\theta_f = 0.357839$  and  $p_{\rho f} = 0$ . The first figure represents the extremal trajectory solution of the continuation problem for  $\gamma_- = 0.1$ ;  $p_\phi(0)$ ,  $p_\rho(0)$  and  $t_f$  are, respectively, plotted in solid, dashed and dotted lines.

## 7.2. The integrable case

In this case, we fix the final purity  $\rho_f$ . To simplify the computations, we use the cyclic coordinate  $r$  and the constant of motion  $p_r$ . The target state is here given by  $(r_f, \theta_f, \phi_f)$ . Some problems of accessibility have been encountered even for small control durations. The evolution of the radial coordinate is very sensitive to variations in the dissipative parameters. This induces very large variations of the initial adjoint coordinate  $p_r$  in the continuation method. We have therefore to check that the target state belongs to the accessibility set for every value of the dissipative parameters used in the continuation method. When this condition is satisfied, we have observed no problem of convergence for the continuation method as displayed in Fig. 12. Fig. 13 illustrates the constraint due to the

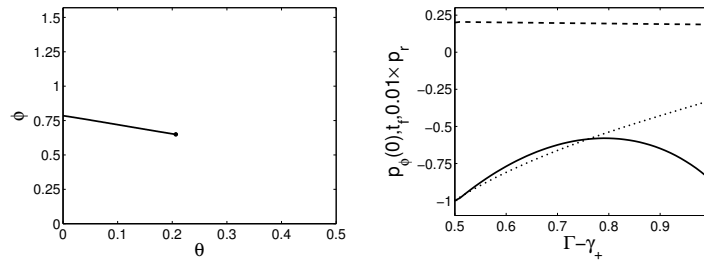


Figure 12. Continuation with respect to  $\Gamma - \gamma_+$ . The parameters of the initial point are  $\Gamma = 2.5$ ,  $\gamma_+ = 2$ ,  $\gamma_- = 0$ ,  $\phi(0) = \pi/4$ ,  $p_r = -100$ ,  $p_\theta = 8$  and  $p_\phi(0) = -1$ . The initial time is  $t_f = 0.3236$ . The target state is  $(r_f = -0.454, \phi_f = 0.64933, \theta_f = 0.2065)$ . The first figure represents the extremal trajectory solution of the continuation problem for  $\Gamma - \gamma_+ = 1$ ;  $p_\phi(0)$ ,  $t_f$  and  $p_r/100$  are, respectively, plotted in solid, dashed and dotted lines.

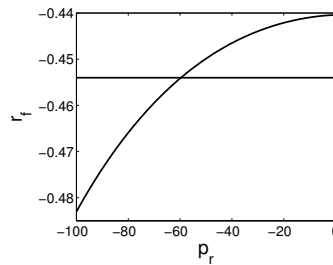


Figure 13. Plot of  $r_f$  as a function of  $p_r$  for  $\Gamma = 2.75$ ,  $\gamma_+ = 2$  and  $\gamma_- = 0$ . Other parameters are taken to be  $\phi(0) = \pi/4$ ,  $p_\theta = 8$ ,  $\phi_f = 0.64933$  and  $\theta_f = 0.2065$ . The equation of the horizontal line is  $r_f = -0.454$ , which corresponds to the target state.

accessibility set. For given values of the dissipative parameters and of  $p_r$ , we have determined the values of  $p_\phi(0)$  and  $t_f$ , which allow for reaching the point of coordinates  $(\phi_f, \theta_f)$ . We have then plotted the corresponding radial coordinate  $r_f$  as a function of  $p_r$ . Note that the diagram is symmetric with respect to the vertical axis  $p_r = 0$  and has roughly the same form up to vertical translation for different values of the dissipative parameters. Fig. 13 shows the values of the radial coordinate  $r_f$  that can be reached when  $\phi_f$  and  $\theta_f$  are fixed. Using such a diagram for different dissipative parameters, one can control that the point  $(r_f, \phi_f, \theta_f)$  belongs to the accessibility set. This diagram gives also an approximative value for  $p_r$ , which can be used in the continuation method.

### 7.3. The generic case

We have done the same work as for the integrable case. The adjoint coordinate  $p_r$  is no more a constant. The role of  $p_r$  is here played by  $p_\rho(0)$  in Figs. 14 and 15. We have considered a continuation as a function of  $\gamma_-$  in Fig. 14. We have observed no effect of the bifurcation in  $\gamma_- = 0$ . Very short durations have been chosen to avoid controllability problems. In Fig. 14, note the strong variations of  $p_\phi(0)$  and  $p_\rho(0)$  when  $\gamma_-$  is varied, which explains the numerical sensitivity of the continuation method.

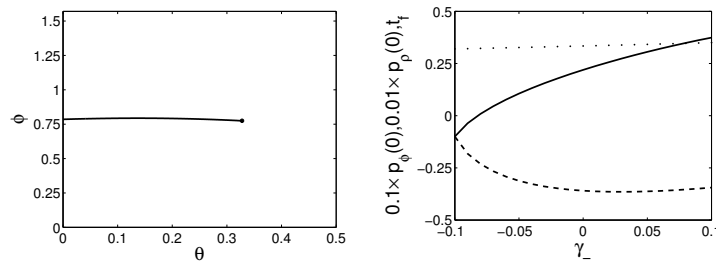


Figure 14. Continuation with respect to  $\gamma_-$ . The parameters of the initial point are  $\Gamma = 2.5$ ,  $\gamma_+ = 2$ ,  $\gamma_- = -0.1$ ,  $\phi(0) = \pi/4$ ,  $p_\rho = -10$ ,  $p_\theta = 8$  and  $p_\phi(0) = -1$ . The initial time is  $t_f = 0.32$ . The target state corresponds to  $\phi_f = 0.77468$ ,  $\theta_f = 0.32774$  and  $\rho_f = 0.47182$ . The first figure represents the extremal trajectory solution of the continuation problem for  $\gamma_- = 0.1$ ;  $p_\phi(0)/10$ ,  $t_f$  and  $p_\rho(0)/100$  are, respectively, plotted in black, dashed and dotted lines.

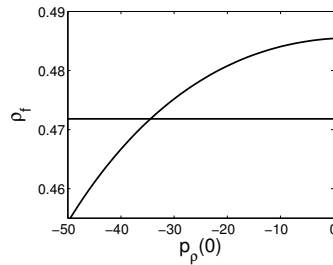


Figure 15. Plot of  $\rho_f$  as a function of  $p_\rho(0)$  for  $\Gamma = 2.5$ ,  $\gamma_+ = 2$  and  $\gamma_- = 0.1$ . Other parameters are taken to be  $\phi(0) = \pi/4$ ,  $p_\theta = 8$ ,  $\phi_f = 0.77468$  and  $\theta_f = 0.32774$ . The equation of the horizontal line is  $\rho_f = 0.47182$ , which corresponds to the target state.

## 8. Conclusion

The contribution of this article is multiple. First of all, for the analysis of generalized Zermelo navigation problems, we prove that first and second order necessary and sufficient conditions allow for deducing a smooth Hamiltonian vector

field concentrating the optimality analysis into a geometric study of the corresponding flow. Optimality is recovered from the behavior of the trajectories through the geometric concept of conjugate point, which can be numerically checked. Moreover, non smooth solutions can be deduced from a singularity analysis of the singular flow near the switching surface. Applied to our problem, this general framework is successfully used to make the study. We found geometric coordinates, which in this case are simply the spherical coordinates  $(\rho, \phi, \theta)$ . Non-smooth optimal curves are deduced, mainly for the problem of controlling the system with a real laser field. In this simplified problem the maximum principle is crucial to compute the switching rules. For the complete problem, since the system depends upon three dissipative parameters, we have presented the analysis using a continuation method on the set of parameters. A rough geometric model is the Grushin one on a two-sphere of revolution. By making a continuation from this starting point, we detect a bifurcation, where non compactness of the adjoint vector component  $p_\phi$  is observed. This allows for making a general analysis, where the behavior of the extremal flow is classified by its asymptotic properties only. Combined with numerical simulations to check the second-order optimality we only find in the generic case two types of optimal trajectories. This gives a complete physical answer to the optimal control of the two-level dissipative case with robustness issues, analyzed using a continuation method. A rather optimistic answer can be found for control of more realistic systems, where the number of levels is about 20 (hence with a state space of dimension 399), as encountered in the experimental project CoMoc.

## References

- ALLGOWER, E. and GEORG. K. (1990) *Numerical Continuation Methods: An Introduction*. Springer-Verlag, New York.
- ALTAFINI, C.A. (2002) Controllability properties for finite dimensional quantum Markovian master equations. *J. Math. Phys.* **44**, 2357–2372.
- BAO, D., ROBLES, C. and SHEN, Z. (2004) Zermelo navigation on Riemannian manifolds. *J. Differential Geom.* **66** (3), 377–435.
- BONNARD, B., CAILLAU, J.-B. and TRÉLAT, E. (2007) Second-order optimality conditions in the smooth case and applications in optimal control. *ESAIM : COCV*. **13**, 2, 207–236.
- BONNARD, B., CAILLAU, J.-B., SINCLAIR, R. and TANAKA, M. (2009) Conjugate and cut loci of a two-sphere of revolution with application to optimal control. *Ann. Inst. H. Poincaré Anal. Non Linéaire* **26**, 1081–1098.
- BONNARD, B. and CHYBA, M. (2003) *Singular Trajectories and Their Role in Control Theory*. Mathématiques & Appl. **40**. Springer-Verlag, Berlin.
- BONNARD, B., CHYBA, M. and SUGNY, D. (2009) Time-minimal control of dissipative two-level quantum systems: the generic case. *IEEE Trans. AC.*, **54** (11), 2598–2610.

- BONNARD, B. and KUPKA, I. (1993) Théorie des singularités de l'application entrée/sortie et optimalité des trajectoires singulières dans le problème du temps minimal. *Forum Mathematicum* **5**, 111–159.
- BONNARD, B. and SUGNY, D. (2008) Optimal control theory with applications in space and quantum dynamics. *AIMS. Series in Applied Math.*, submitted.
- BONNARD, B. and SUGNY, D. (2009a) Time-minimal control of dissipative two-level quantum systems: the integrable case. *SIAM J. Control Optim.* **48** (3), 1289–1308.
- BONNARD, B. and SUGNY, D. (2009b) Optimal control theory with applications in space and quantum mechanics. *AIMS. Series in Applied Maths.*, submitted.
- BOSCAIN, U. and PICCOLI, B. (2004) *Optimal Syntheses for Control Systems on 2-D Manifolds. Mathématiques & Applications* **43**. Springer-Verlag, Berlin.
- BOSCAIN, U. et al. (2002) Optimal control in laser-induced population transfer for two- and three-level quantum systems. *J. Math. Phys.* **43** (5), 2107.
- CARATHÉODORY, C. (1982) *Calculus of Variations and Partial Differential Equations of First Order*. Chelsea Publishing company, New-York.
- COTCOT *Conditions of Order Two: Conjugate Times*. <http://apo.enseiht.fr/cotcot>.
- EKELAND, I. (1978) Discontinuités de champs hamiltoniens et existence de solutions optimales en calcul des variations. *Inst. Hautes Etudes Sci. Publ. Math.* **47**, 5–32.
- GORINI, V., KOSSAKOWSKI, A. and SUDARSHAN, E.C.G. (1976) Completely positive dynamical semigroups of  $N$ -level systems. *J. Math. Phys.* **17**, 821–825.
- KHANEJA, N., BROCKETT, R.W. and GLASER, S.J. (2001) Time optimal control of spin systems. *Phys. Rev. A* **63**, 032308.
- KHANEJA, N., GLASER, S.J. and BROCKETT, R.W. (2002) Sub-Riemannian geometry and time optimal control of three spin systems: Coherence transfer and quantum gates. *Phys. Rev. A* **65**, 032301.
- KOSSAKOWSKI, A. (1973) On the general form of the generator of a dynamical semi-group for the spin 1/2 system. *Bull. Acad. Pol. Sciences, Ser. Sciences Math., Ast., Phys.* **21**, 7, 649–653.
- LEE, E. and MARKUS, L. (1967) *Foundations of Optimal Control Theory*. John Wiley, New York.
- LINDBLAD, G. (1976) On the generators of quantum dynamical semi-groups. *Comm. Math. Phys.* **48**, 119.
- PONTRYAGIN, L. et al. (1961) *The Mathematical Theory of Optimal Processes*. John Wiley, New York.
- SUGNY, D., KONTZ, C. and JAUSLIN, H.R. (2007) Time-optimal control of two-level dissipative quantum systems. *Phys. Rev. A* **76**, 023419.
- VIEILLARD, T. et al. (2008) Field-free molecular alignment of  $CO_2$  mixtures in presence of collisional relaxation. *J. Raman Spectrosc.* **39**, 694–699.